

Introduction to Nuclear and Particle Physics

Nuclear structure

Helga Dénes 2023 S2 Yachay Tech

hdenes@yachaytech.edu.ec

Electron scattering

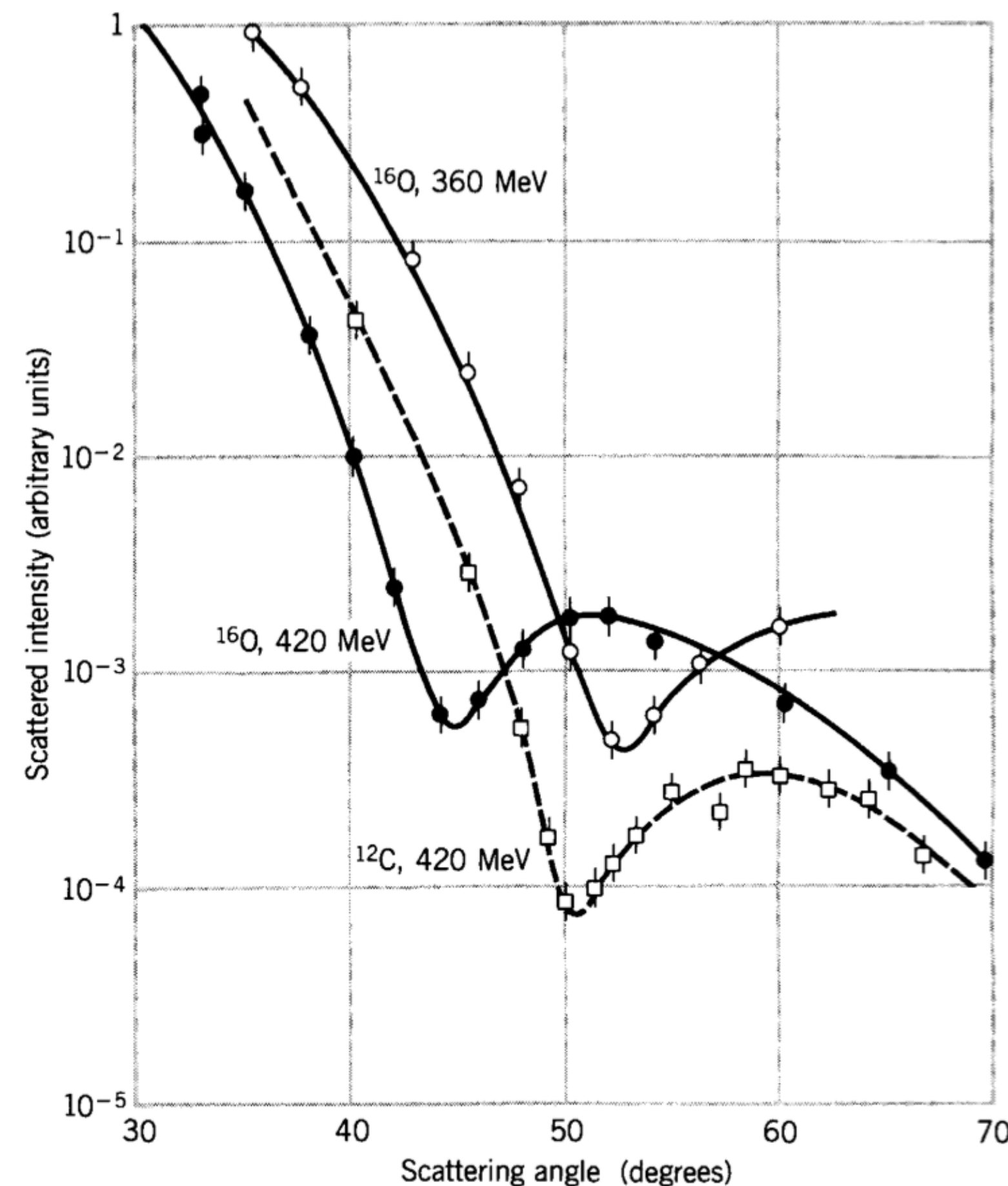


Figure 3.1 Electron scattering from ^{16}O and ^{12}C . The shape of the cross section is somewhat similar to that of diffraction patterns obtained with light waves. The data come from early experiments at the Stanford Linear Accelerator Center (H. F. Ehrenberg et al., *Phys. Rev.* **113**, 666 (1959)).

Electron scattering

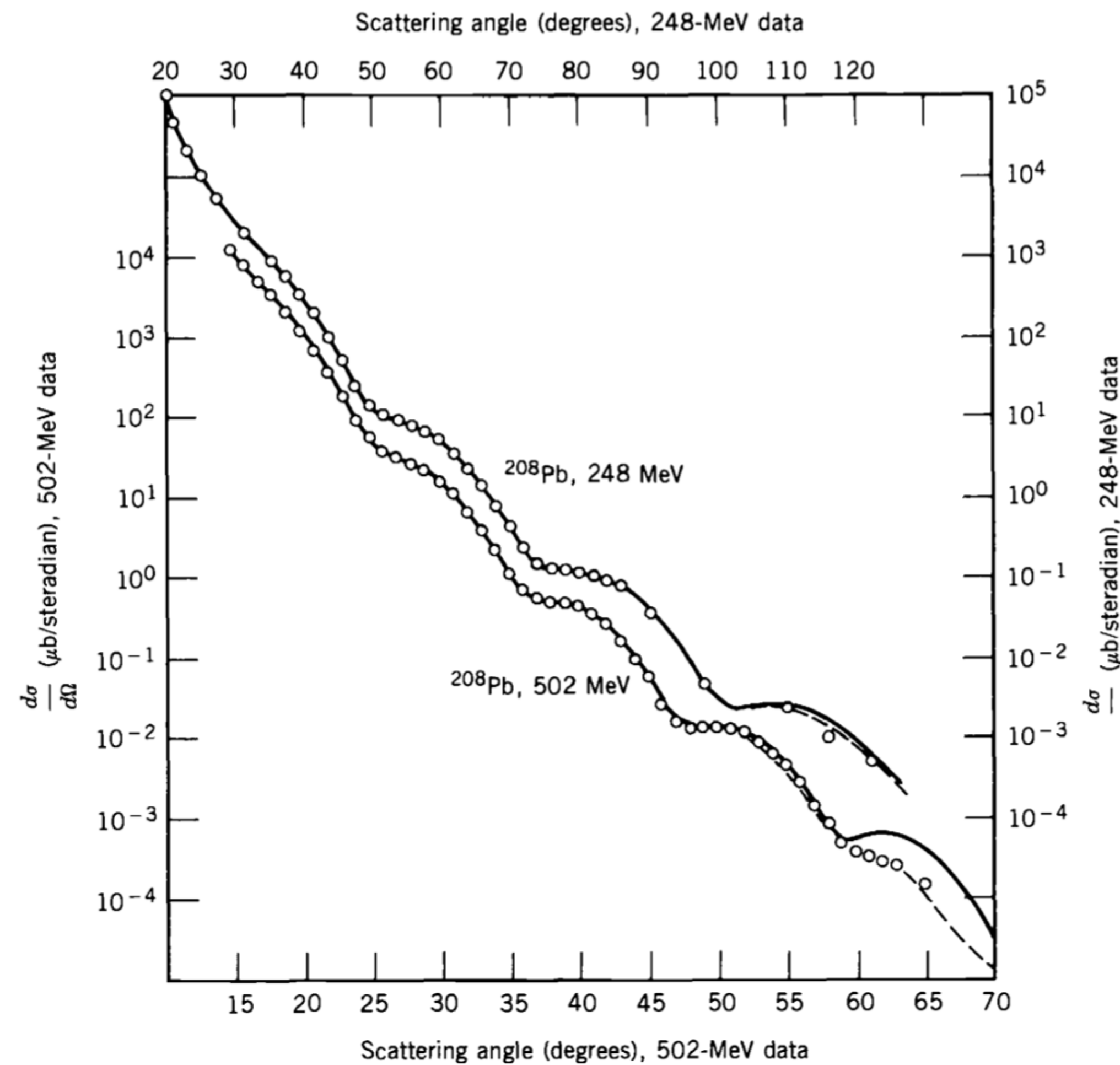


Figure 3.2 Elastic scattering of electrons from ^{208}Pb . Note the different vertical and horizontal scales for the two energies. This also shows diffractionlike behavior, but lacks sharp minima. (J. Heisenberg et al., *Phys. Rev. Lett.* **23**, 1402 (1969).)

Electron scattering

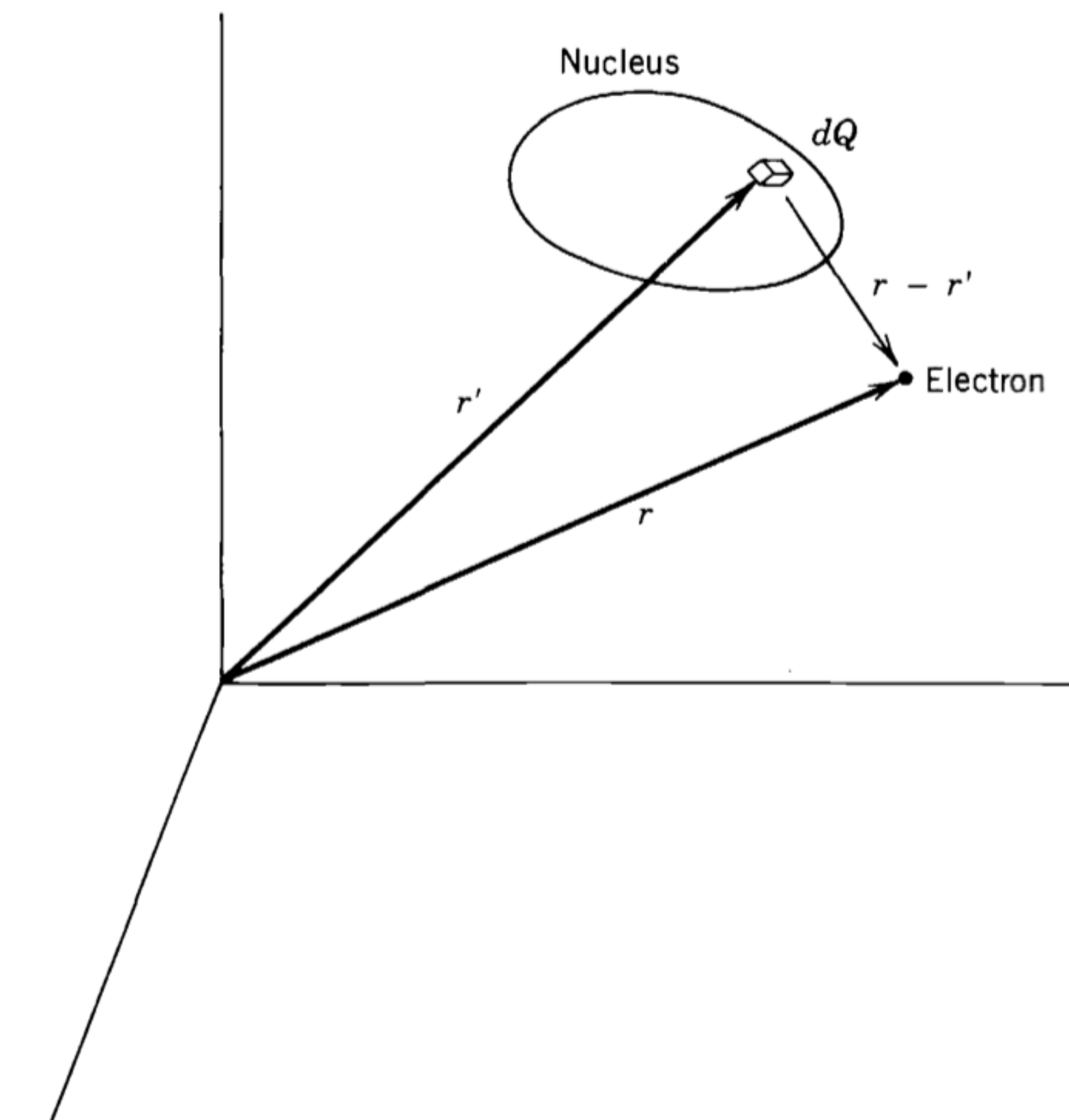


Figure 3.3 The geometry of scattering experiments. The origin of coordinates is located arbitrarily. The vector r' locates an element of charge dQ within the nucleus, and the vector r defines the position of the electron.

Electron scattering

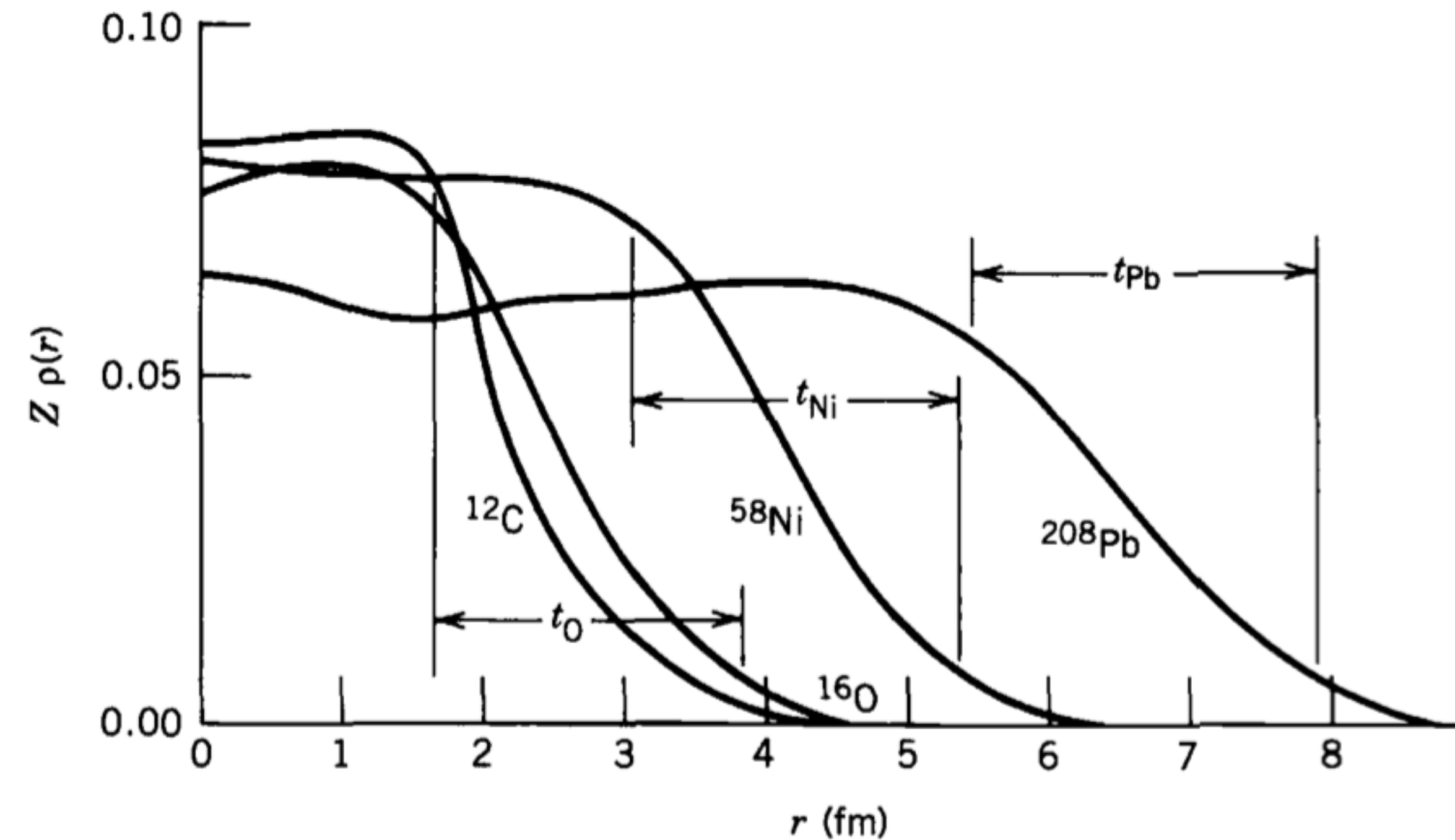


Figure 3.4 The radial charge distribution of several nuclei determined from electron scattering. The skin thickness t is shown for O, Ni, and Pb; its value is roughly constant at 2.3 fm. The central density changes very little from the lightest nuclei to the heaviest. These distributions were adapted from R. C. Barrett and D. F. Jackson, *Nuclear Sizes and Structure* (Oxford: Clarendon, 1977), which gives more detail on methods of determining $\rho(r)$.

Electron scattering

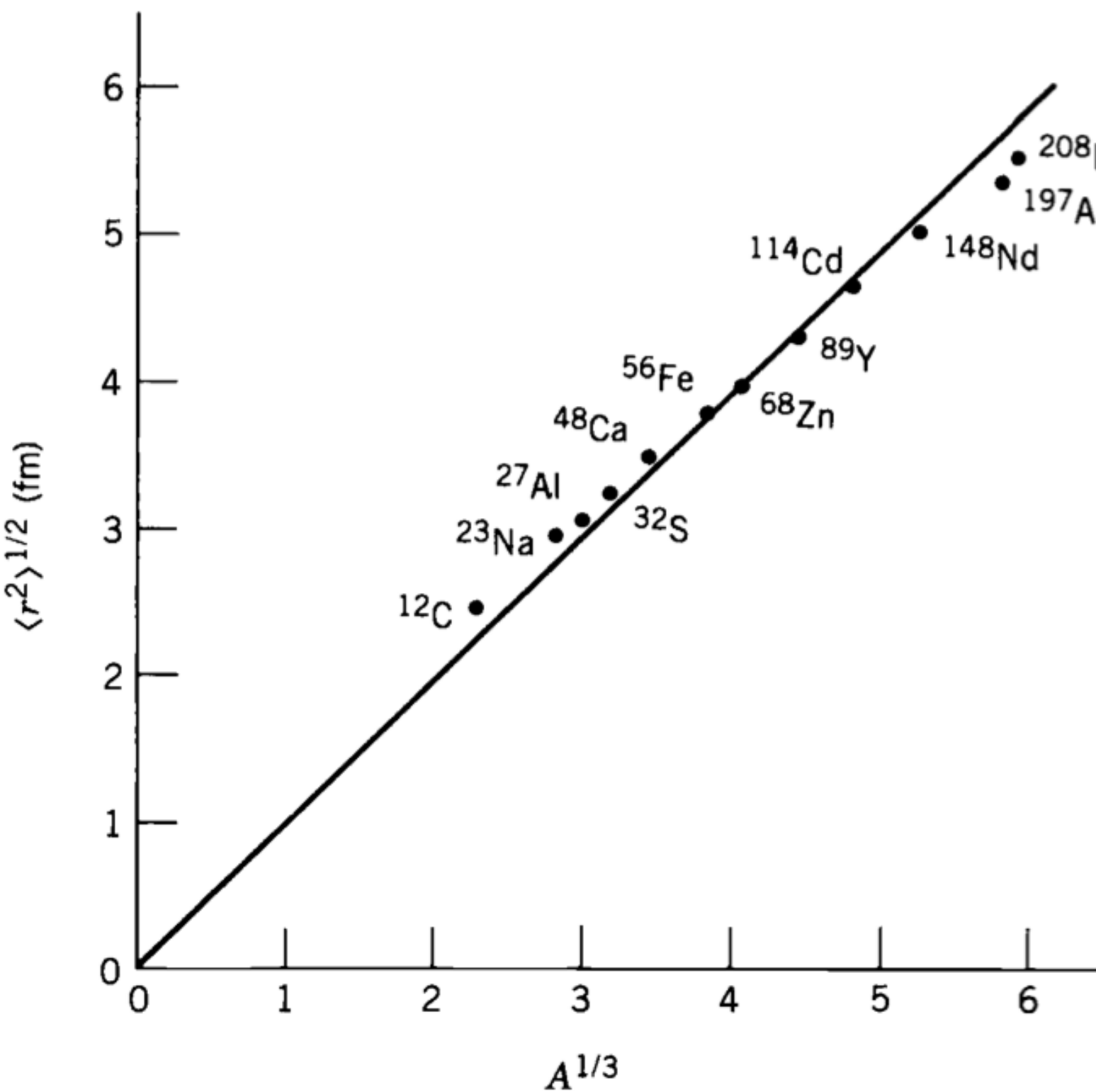


Figure 3.5 The rms nuclear radius determined from electron scattering experiments. The slope of the straight line gives $R_0 = 1.23$ fm. (The line is not a true fit to the data points, but is forced to go through the origin to satisfy the equation $R = R_0 A^{1/3}$.) The error bars are typically smaller than the size of the points (± 0.01 fm). More complete listings of data and references can be found in the review of C. W. de Jager et al., *Atomic Data and Nuclear Data Tables* 14, 479 (1974).

Isotope shift

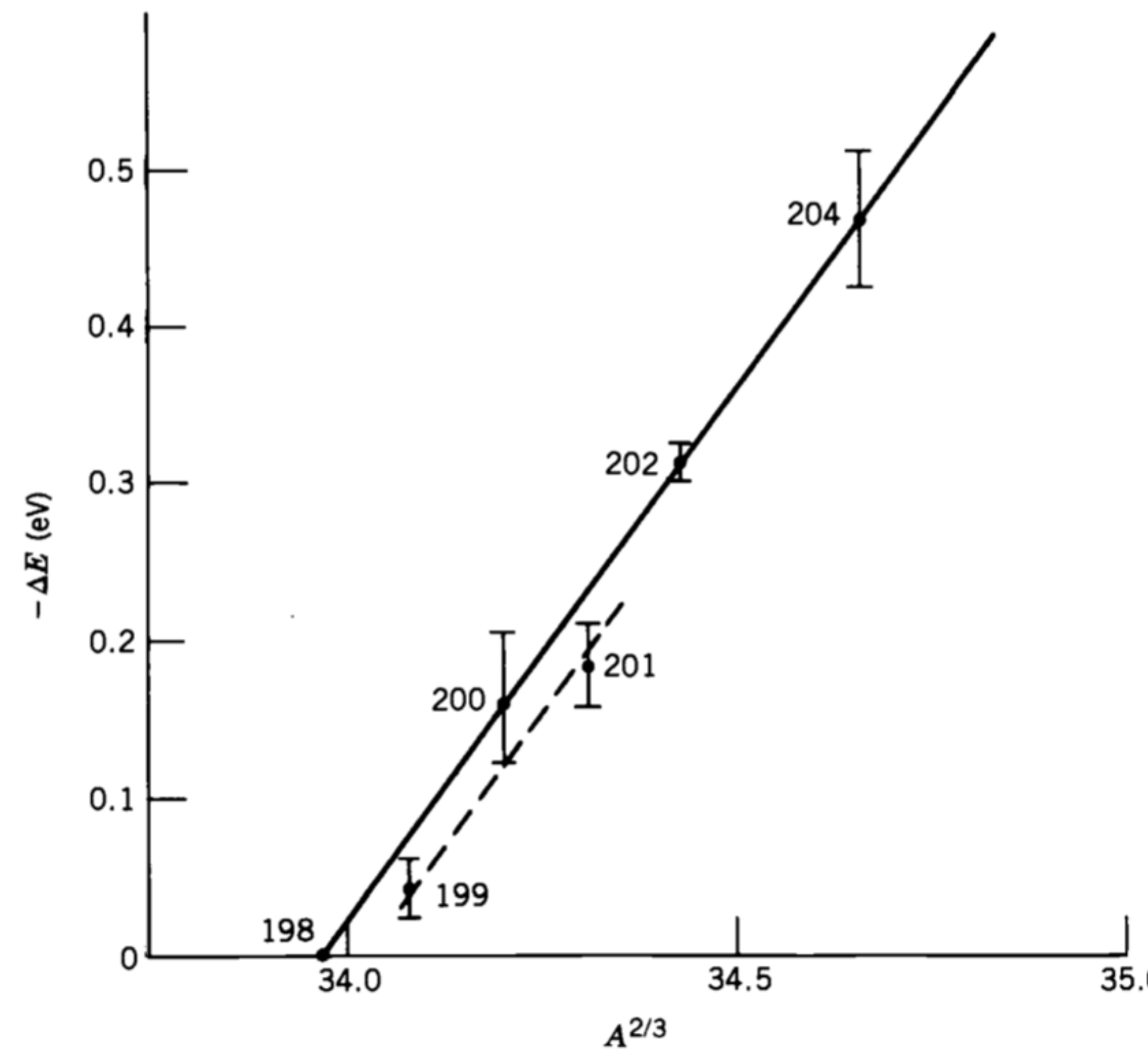


Figure 3.6 K X-ray isotope shifts in Hg. The energy of the K X ray in Hg is about 100 keV, so the relative isotope shift is of the order of 10^{-6} . The data show the predicted dependence on $A^{2/3}$. There is an “odd-even” shift in radius of odd-mass nuclei relative to their even- A neighbors, brought about by the orbit of the odd particle. For this reason, odd- A isotopes must be plotted separately from even- A isotopes. Both groups, however, show the $A^{2/3}$ dependence. The data are taken from P. L. Lee et al., *Phys. Rev. C* 17, 1859 (1978).

Isotope shift

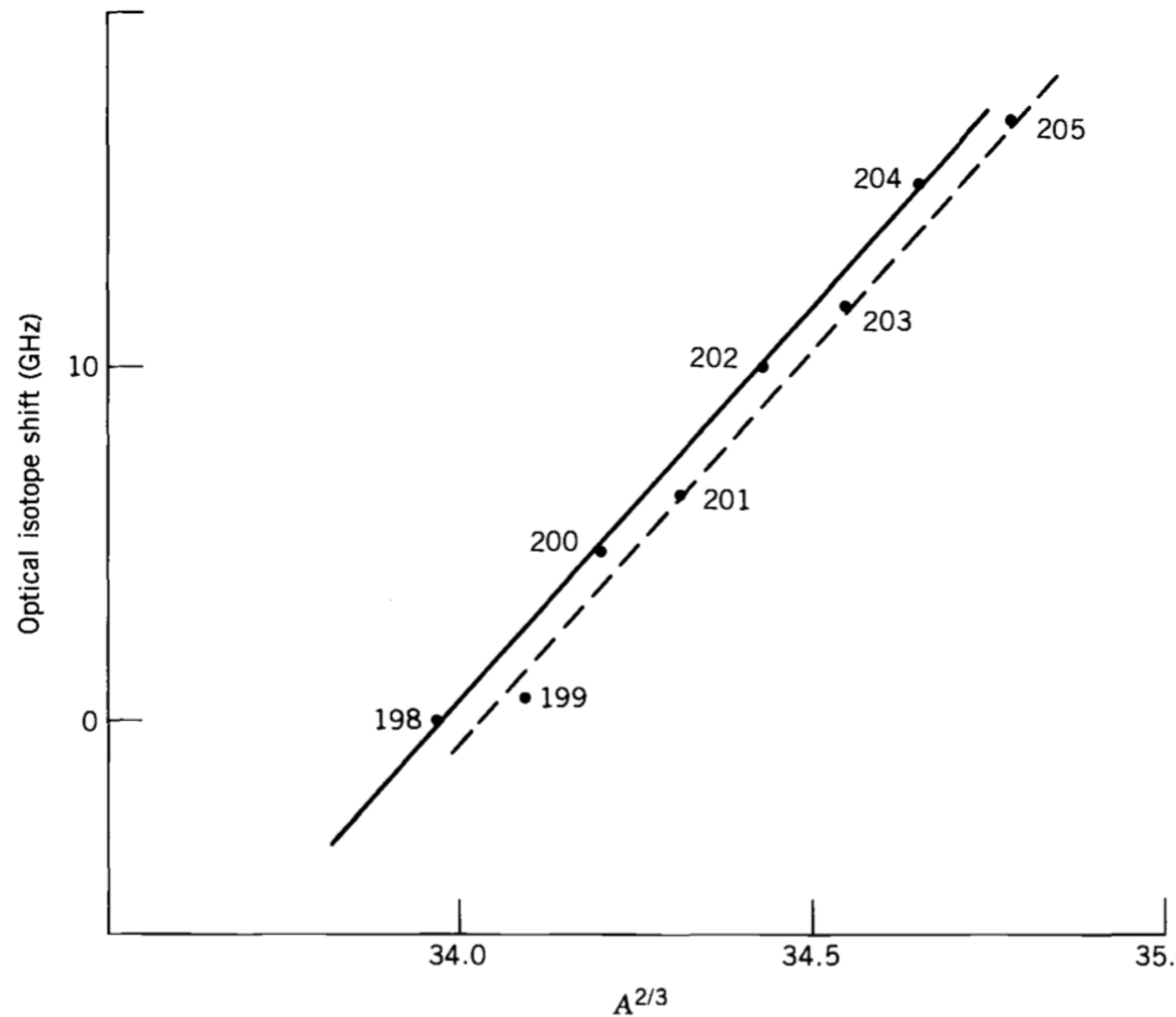


Figure 3.7 Optical isotope shifts in Hg isotopes from 198 to 205, measured relative to 198. These data were obtained through laser spectroscopy; the experimental uncertainties are about $\pm 1\%$. The optical transition used for these measurements has a wavelength of 253.7 nm, and the isotope shift is therefore about one part in 10^7 . Compare these results with Figure 3.6. Data taken from J. Bonn et al., *Z. Phys. A* **276**, 203 (1976).

Isotope shift

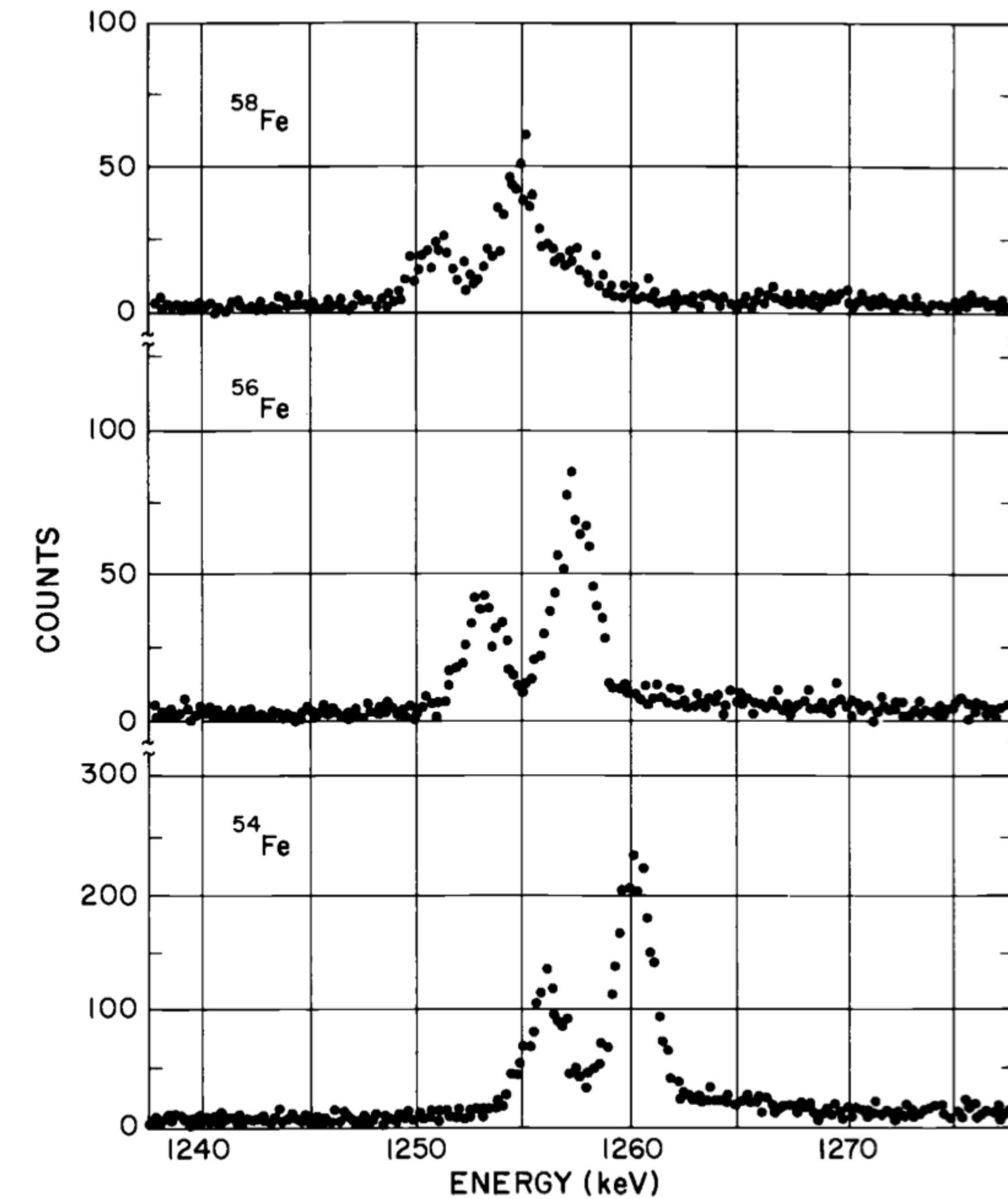


Figure 3.8 The muonic K X rays in some Fe isotopes. The two peaks show the $2\text{p}_{3/2} \rightarrow 1\text{s}_{1/2}$ and $2\text{p}_{1/2} \rightarrow 1\text{s}_{1/2}$ transitions, which have relative intensities in the ratio 2:1 determined by the statistical weight $(2j + 1)$ of the initial state. The isotope shift can clearly be seen as the change in energy of the transitions. The effect is about 0.4%, which should be compared with the 10^{-6} effect obtained with electronic K X rays (Figure 3.6). From E. B. Shera et al., *Phys. Rev. C* **14**, 731 (1976).

Isotope shift

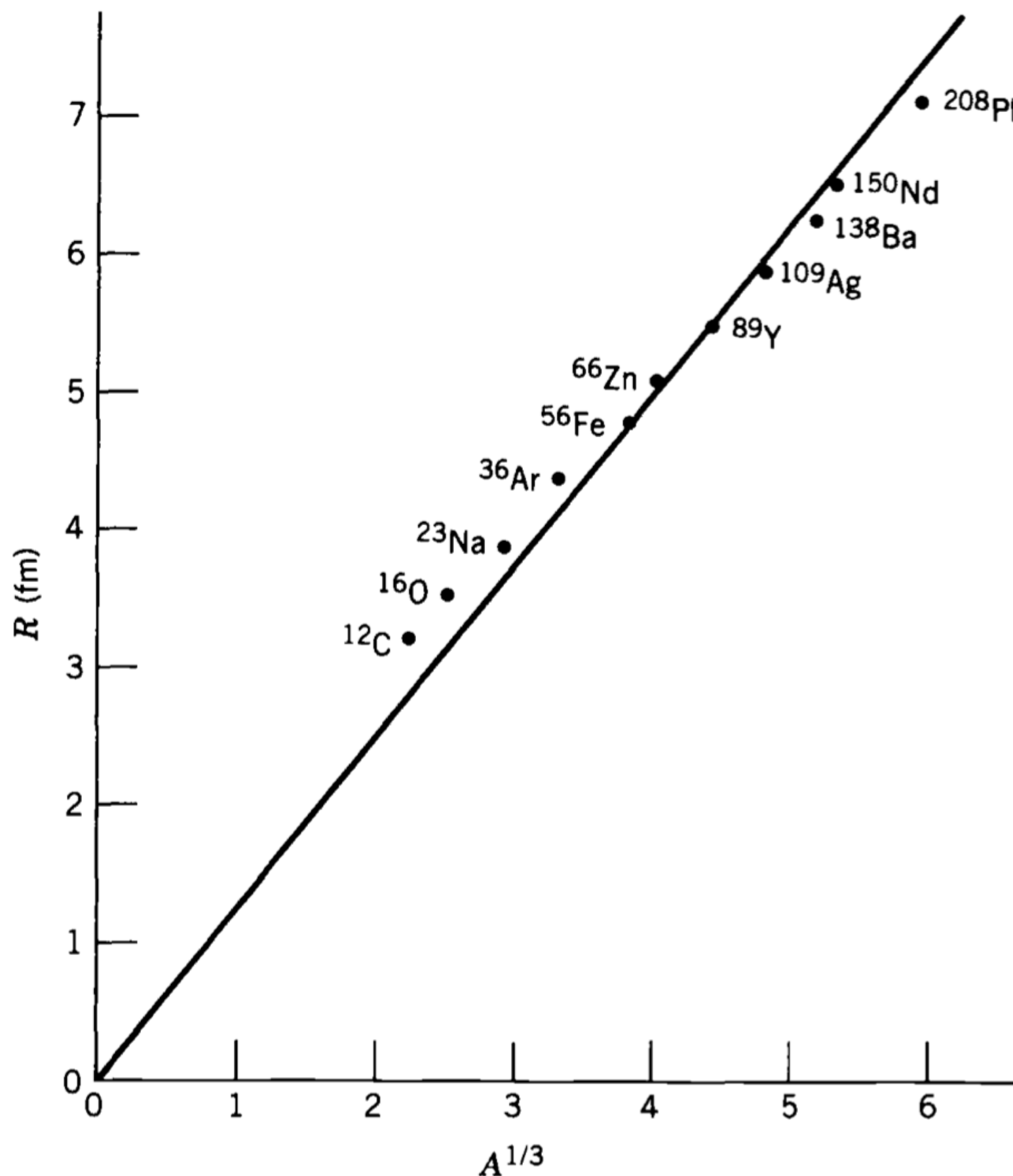


Figure 3.9 The mean nuclear radius determined from muonic X-ray measurements. As in Figure 3.5, the data depend roughly linearly on $A^{1/3}$ (again forcing the line to go through the origin). The slope of the line gives $R_0 = 1.25$ fm. The data are taken from a review of muonic X-ray determinations of nuclear charge distributions by R. Engfer et al., *Atomic Data and Nuclear Data Tables* **14**, 509 (1974).

Mirror nuclei

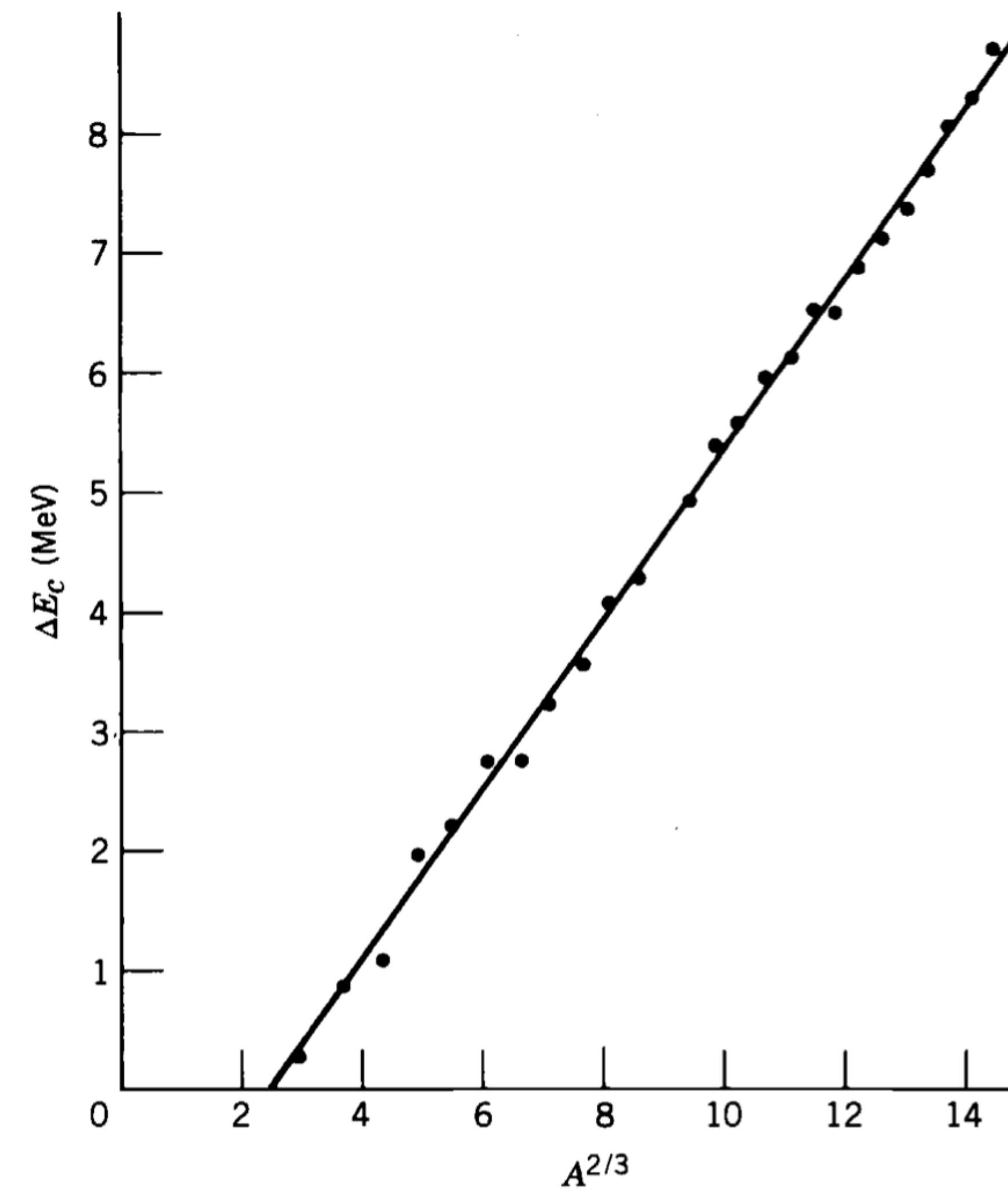


Figure 3.10 Coulomb energy differences of mirror nuclei. The data show the expected $A^{2/3}$ dependence, and the slope of the line gives $R_0 = 1.22$ fm.

He scattering

Low energy scattering

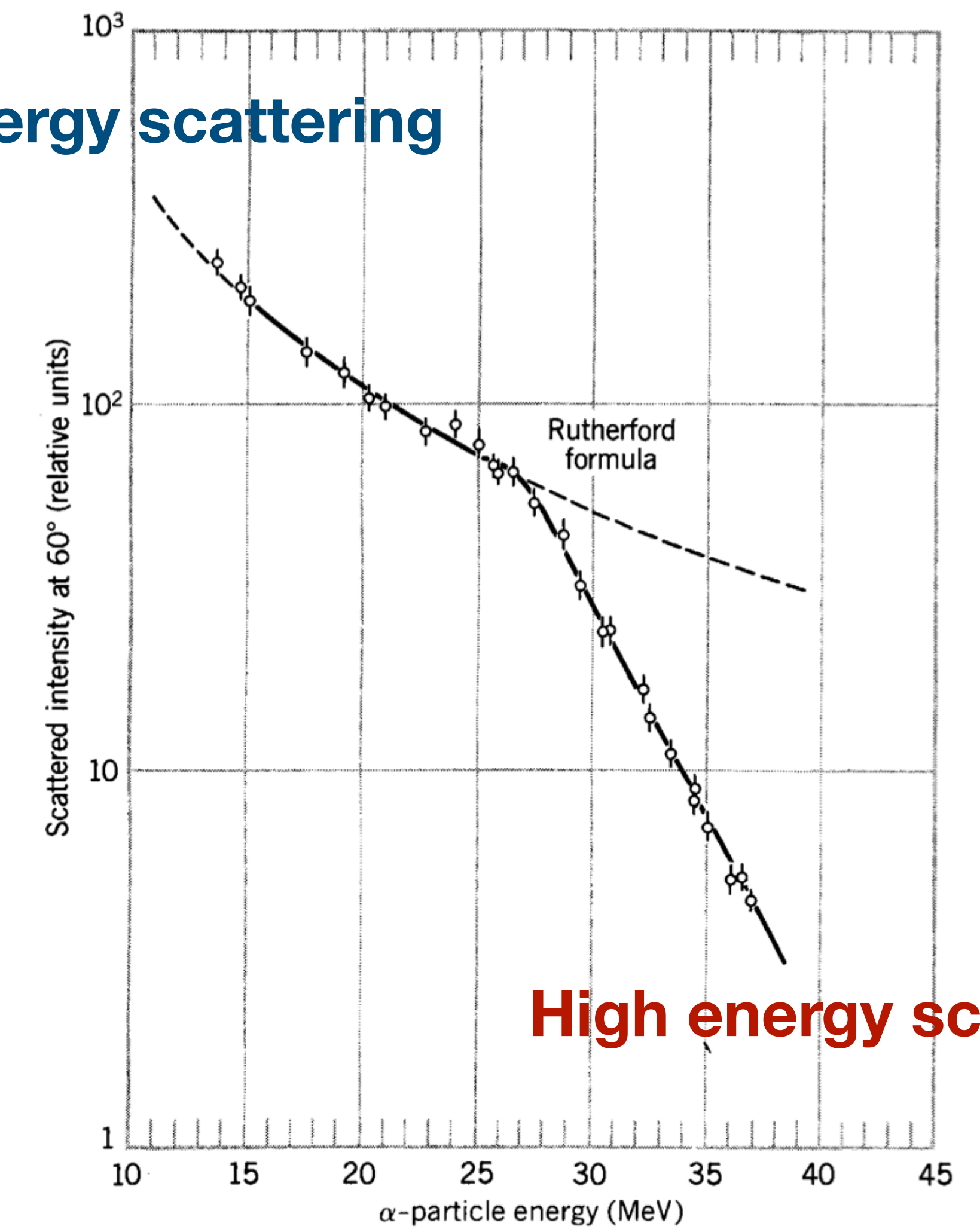


Figure 3.11 The breakdown of the Rutherford scattering formula. When the incident α particle gets close enough to the target Pb nucleus so that they can interact through the nuclear force (in addition to the Coulomb force that acts when they are far apart) the Rutherford formula no longer holds. The point at which this breakdown occurs gives a measure of the size of the nucleus. Adapted from a review of α particle scattering by R. M. Eisberg and C. E. Porter, *Rev. Mod. Phys.* **33**, 190 (1961).

Atomic mass table

```

1      a0dsskgw
0
0      ****
* file : mass.mas20 *
*****
This is one file out of a series of 3 files published in:
"The Ame2020 atomic mass evaluation (I)" by W.J.Huang, M.Wang, F.G.Kondev, G.Audi and S.Naimi
Chinese Physics C45, 030002, March 2021.
"The Ame2020 atomic mass evaluation (II)" by M.Wang, W.J.Huang, F.G.Kondev, G.Audi and S.Naimi
Chinese Physics C45, 030003, March 2021.
for files : mass.mas20 : atomic masses
rct1.mas20 : react and sep energies, part 1
rct2.mas20 : react and sep energies, part 2
A fourth file is the "Rounded" version of the atomic mass table (the first file)
massround.mas20 atomic masses "Rounded" version

Values in files 1, 2 and 3 are unrounded version of the published ones
Values in file 4 are exact copy of the published ones

col 1      : Fortran character control: 1 = page feed  0 = line feed
format     : a1,i3,i5,i5,i5,1x,a3,a4,1x,f14.6,f12.6,f13.5,1x,f10.5,1x,a2,f13.5,f11.5,1x,i3,1x,f13.6,f12.6
             cc NZ N Z A el o   mass unc binding unc      B beta unc    atomic_mass unc
Warnings   : this format is not identical to that used in AME2016;
             one more digit is added to the "BINDING ENERGY/A", "BETA-DECAY ENERGY" and "ATOMIC-MASS" values and their uncertainties;
             # in a place of decimal point : estimated (non-experimental) value;
             * in a place of value : the not calculable quantity

.....+....1....+....2....+....3....+....4....+....5....+....6....+....7....+....8....+....9....+....10....+....11....+....12....+....13

```

MASS LIST
for analysis

1N-Z	N	Z	A	EL	O	MASS EXCESS (keV)	BINDING ENERGY/A (keV)	BETA-DECAY ENERGY (keV)	ATOMIC MASS (micro-u)
0 1	1	0	1	n		8071.31806	0.00044	0.0	1 008664.91590 0.00047
-1	0	1	1	H		7288.971064	0.000013	0.0	1 007825.031898 0.000014
0 0	1	1	2	H		13135.722895	0.000015	1112.2831	0.0002 2 014101.777844 0.000015
0 1	2	1	3	H		14949.81090	0.00008	2827.2654	0.0003 3 016049.28132 0.00008
-1	1	2	3	He		14931.21888	0.00006	2572.68044	0.00015 3 016029.32197 0.00006
-3	0	3	3	Li	-pp	28667#	2000#	-2267# 3 030775# 2147#	667# B- *
0 2	3	1	4	H	-n	24621.129	100.000	1720.4491	25.0000 4 026431.867 107.354
0	2	2	4	He		2424.91587	0.00015	7073.9156	0.0002 4 002603.25413 0.00016
-2	1	3	4	Li	-p	25323.190	212.132	1153.7603	53.0330 B- *
									4 027185.561 227.733

Mass spectrograph

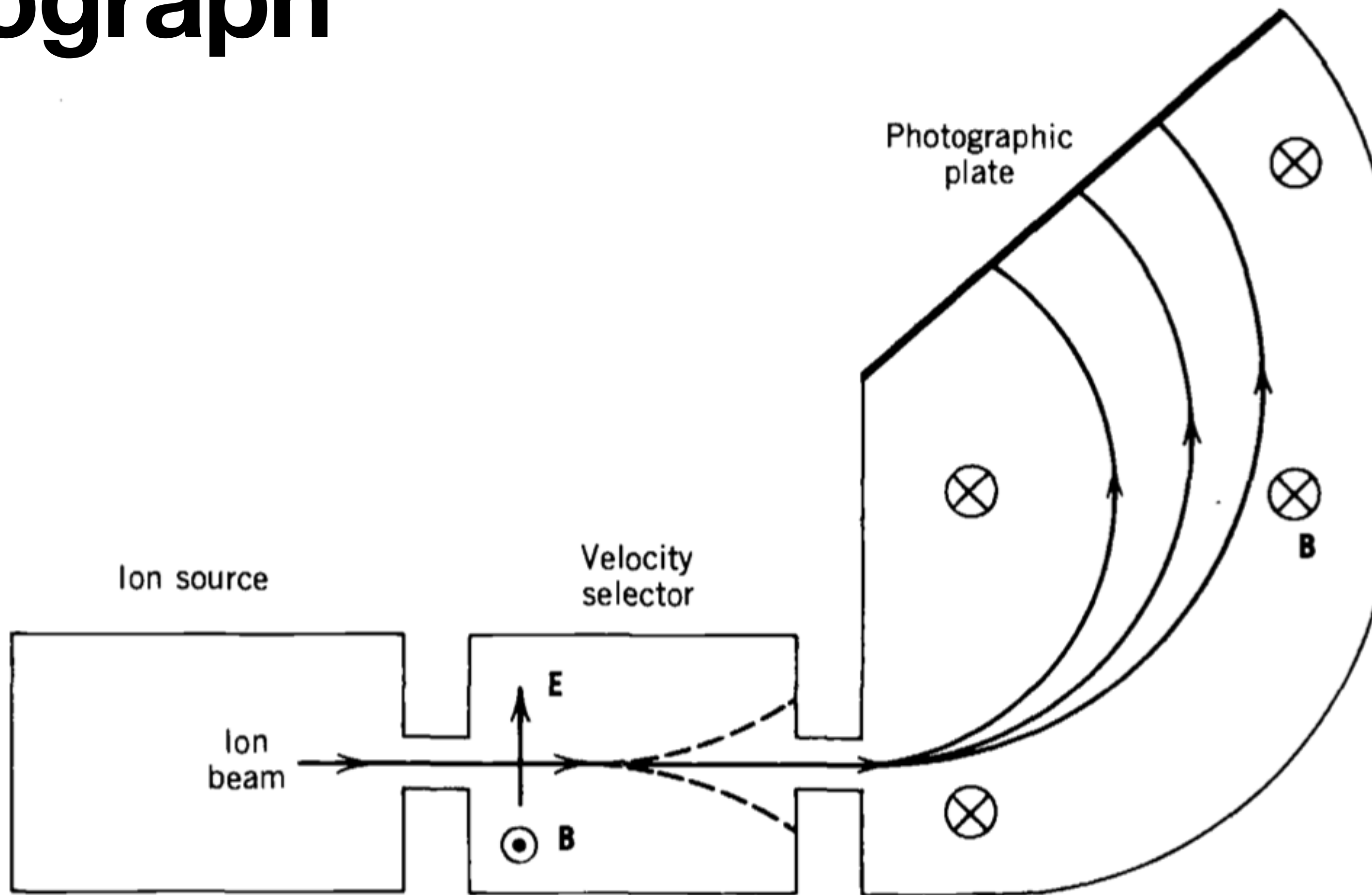
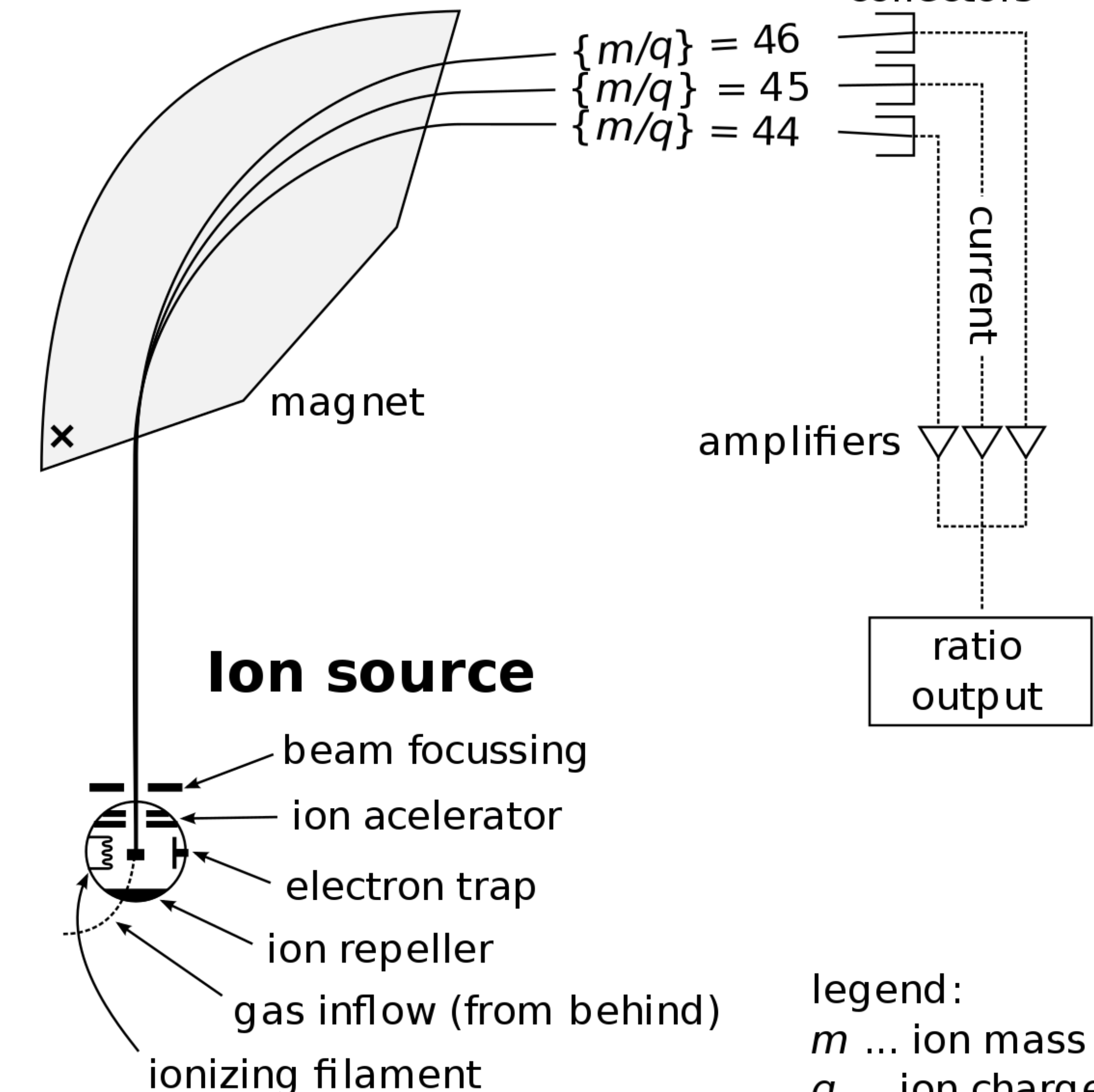


Figure 3.13 Schematic diagram of mass spectrograph. An ion source produces a beam with a thermal distribution of velocities. A velocity selector passes only those ions with a particular velocity (others being deflected as shown), and momentum selection by a uniform magnetic field permits identification of individual masses.

Mass spectrometer

Detection



Mass-spectrum

^{78}Kr 0.356%

^{80}Kr 2.27%

^{82}Kr 11.6%

^{83}Kr 11.5%

^{84}Kr 57.0%

^{86}Kr 17.3%

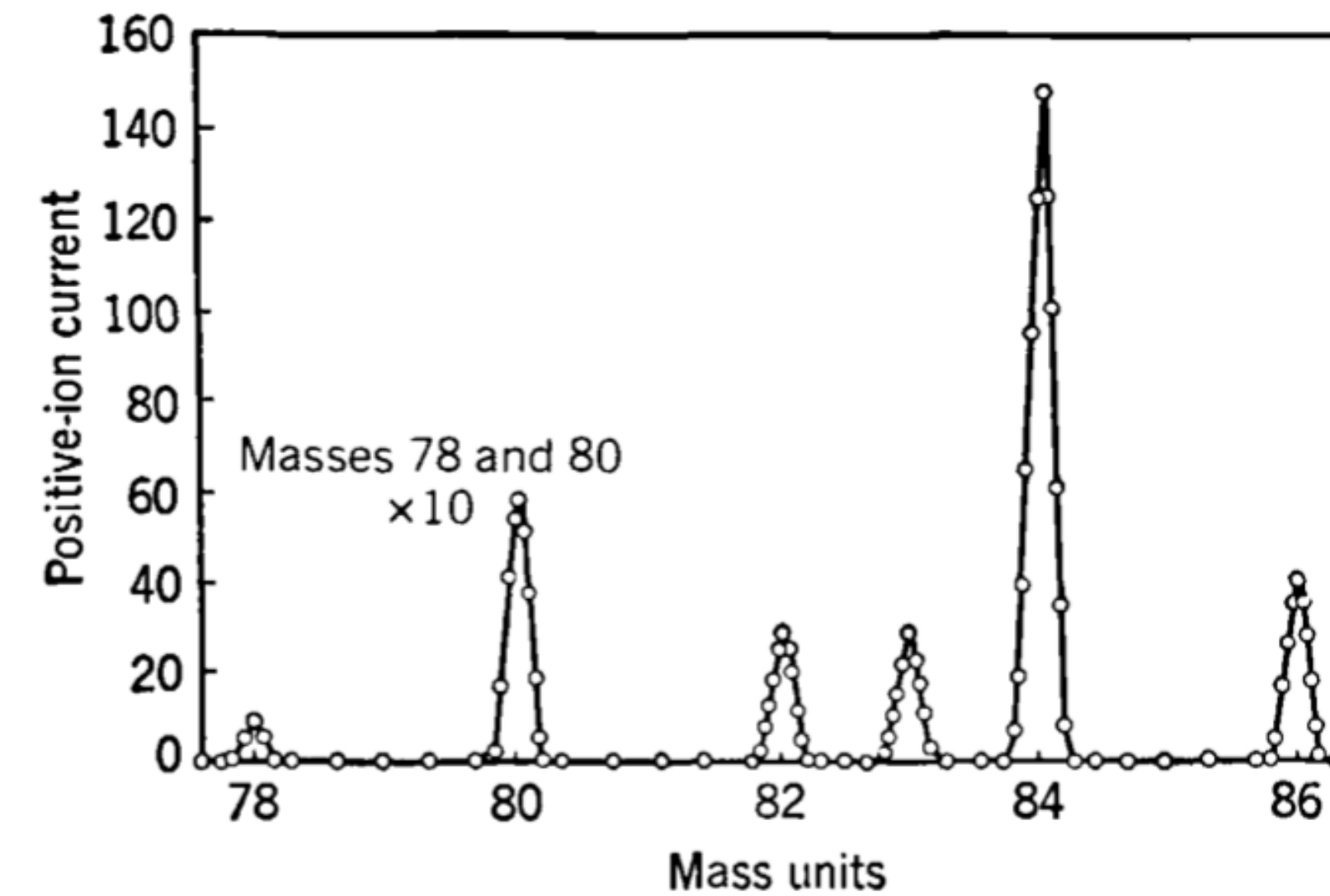


Figure 3.14 A mass-spectrum analysis of krypton. The ordinates for the peaks at mass positions 78 and 80 should be divided by 10 to show these peaks in their true relation to the others.

Kr Isotopes that are not listed are too unstable to be measured with a mass spectrometer (e.g. ^{79}Kr , ^{81}Kr , ^{85}Kr)

Nuclear binding energy

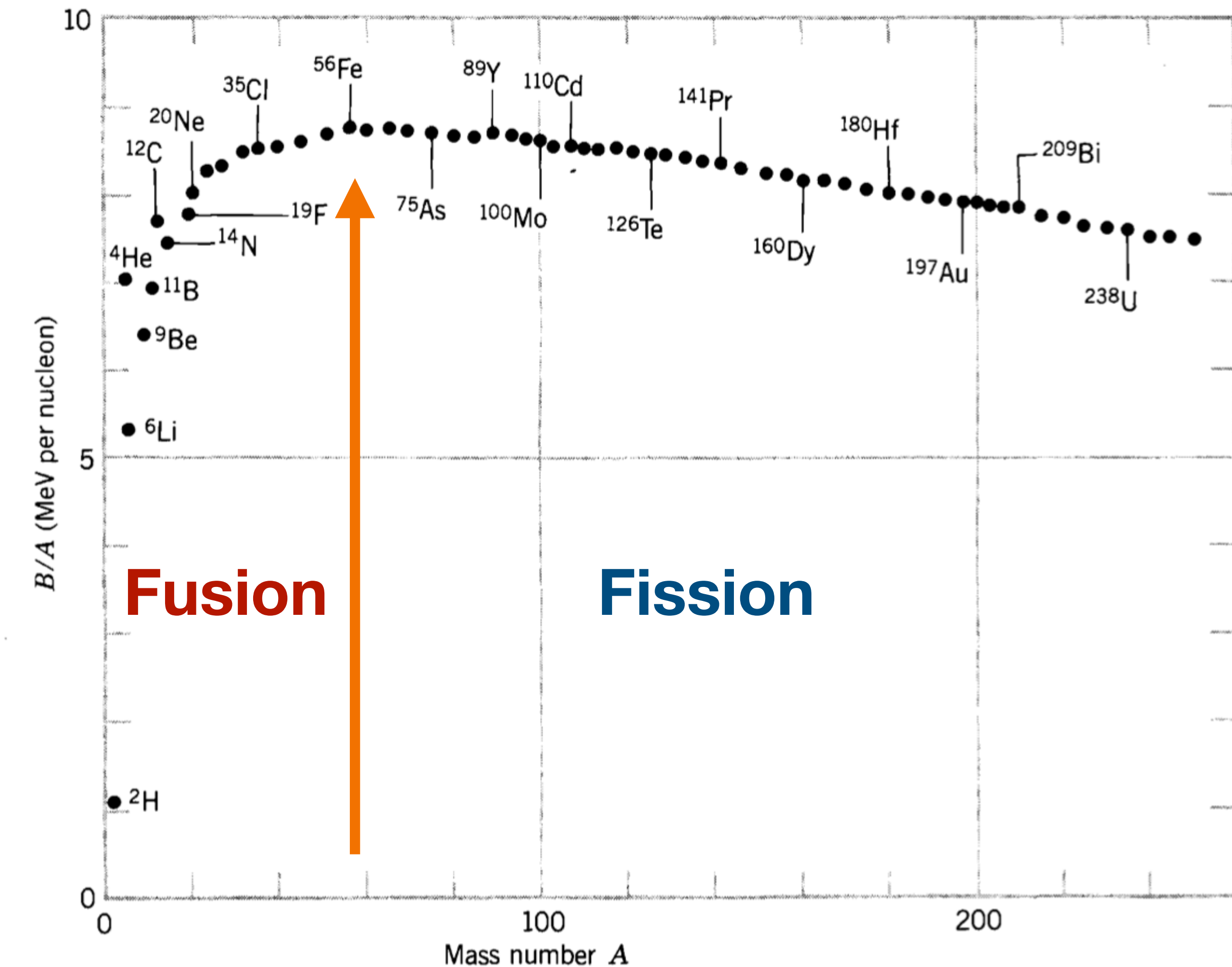


Figure 3.16 The binding energy per nucleon.

Laser Isotop separation

- To separate different isotopes
- Isotopes have slightly different excitation energies -> isotope shift
- If we have a beam with different isotopes
 - Laser 1 has a specific frequency to excite one of the isotopes
 - Laser 2 ionises the already excited atoms
 - The ionised isotopes can be deflected and collected

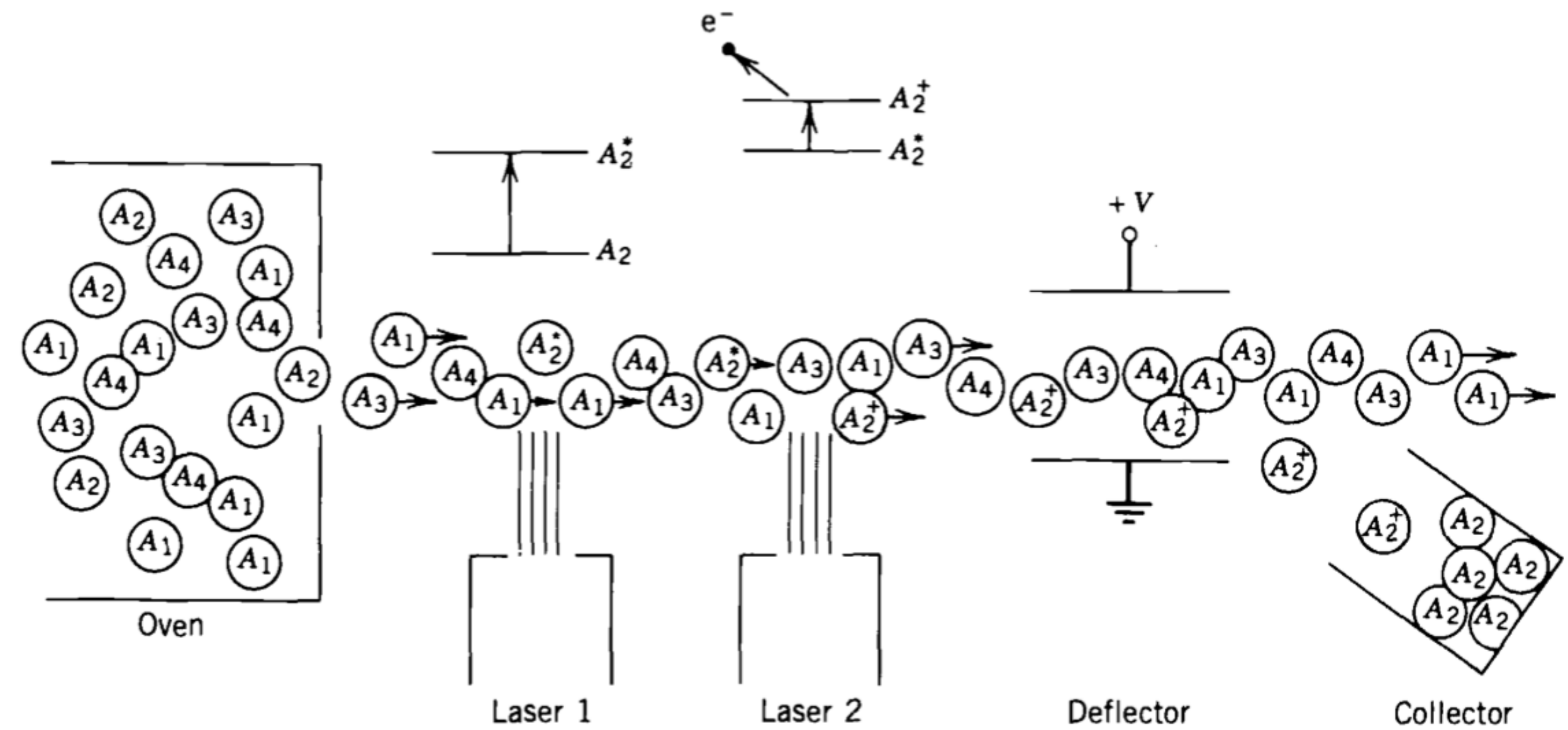
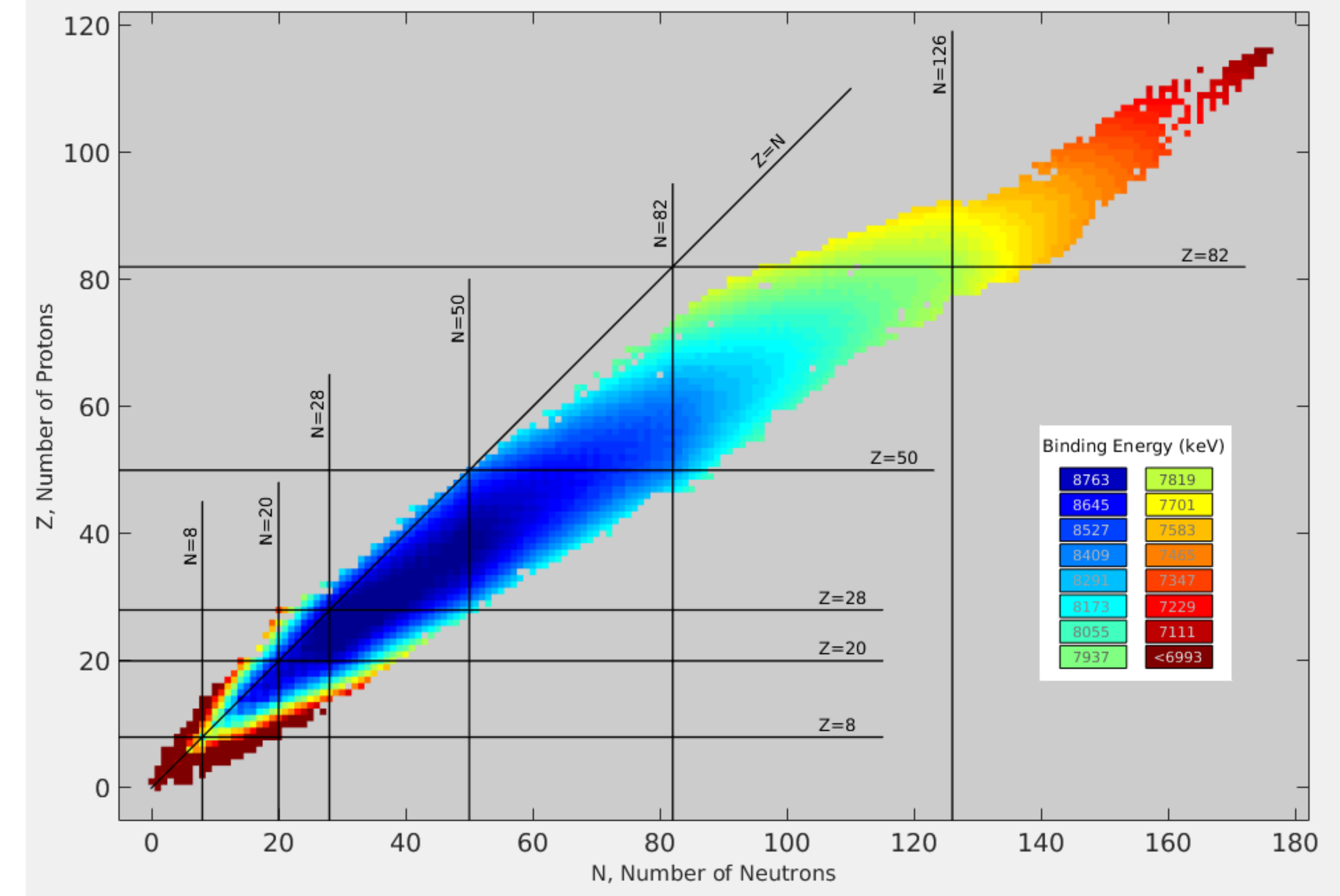


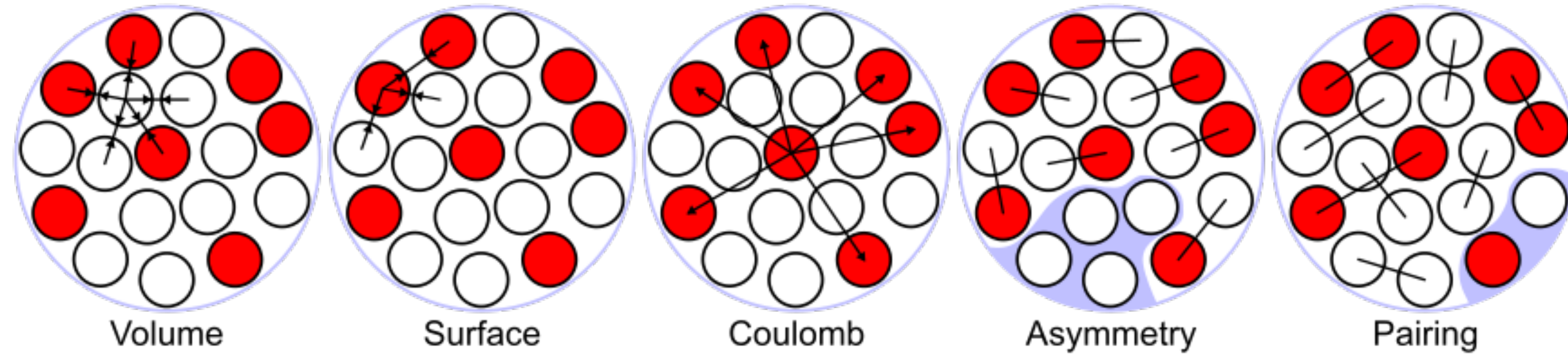
Figure 3.15 Laser isotope separation. The beam of neutral atoms from the oven is a mixture of four isotopes A_1 , A_2 , A_3 , and A_4 . The first laser is tuned to the transition corresponding to the resonant excitation of isotope A_2 to a certain excited state; because of the sharpness of the laser energy and the isotope shift that gives that particular transition a different energy in the other isotopes, only A_2 is excited. The second laser has a broad energy profile, so that many free-electron states can be reached in the ionization of the atoms; but because only the A_2 isotopes are in the excited state, only the A_2 atoms are ionized. The A_2 ions are then deflected and collected.

Binding energy



- Chart of nuclides (isotopes) by **binding energy**, depicting the **valley of stability**.
- The diagonal line corresponds to equal numbers of neutrons and protons.
- Dark **blue squares represent nuclides with the greatest binding energy**, hence they correspond to the most stable nuclides.
- The binding energy is greatest along the floor of the valley of stability.

Semi empirical mass formula - binding energy



1. **Volume energy**, when an assembly of nucleons of the same size is packed together into the smallest volume, each interior nucleon has a certain number of other nucleons in contact with it. So, this nuclear energy is proportional to the volume.
2. **Surface energy** corrects for the previous assumption made that every nucleon interacts with the same number of other nucleons. This term is negative and proportional to the surface area, and is therefore roughly equivalent to liquid surface tension.
3. **Coulomb energy**, the potential energy from each pair of protons. As this is a repulsive force, the binding energy is reduced.
4. **Asymmetry energy** (also called Pauli energy), which accounts for the Pauli exclusion principle. Unequal numbers of neutrons and protons imply filling higher energy levels for one type of particle, while leaving lower energy levels vacant for the other type.
5. **Pairing energy**, which accounts for the tendency of proton pairs and neutron pairs to occur. An even number of particles is more stable than an odd number due to spin coupling.

Nuclear binding energy

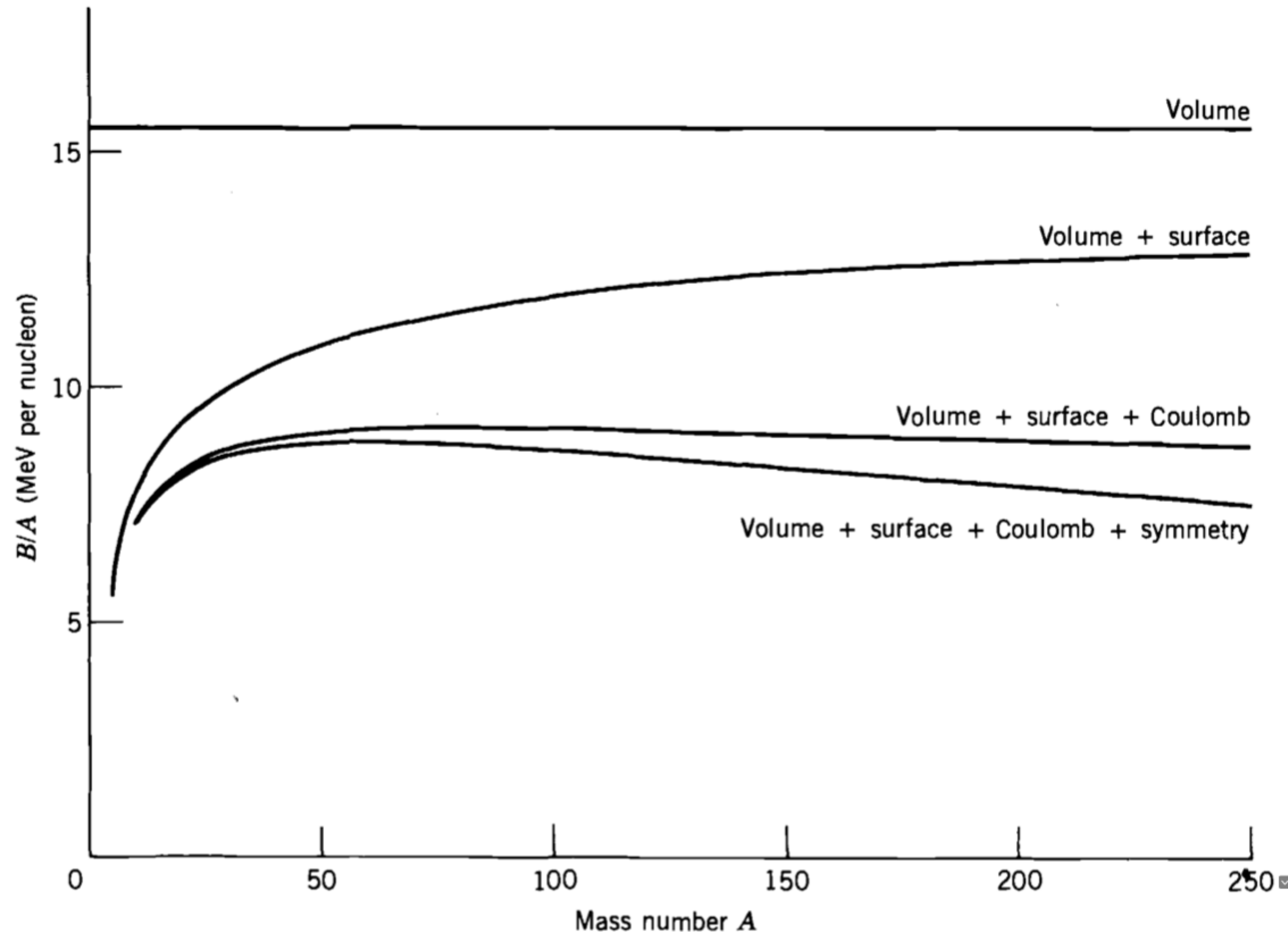


Figure 3.17 The contributions of the various terms in the semiempirical mass formula to the binding energy per nucleon.

Nuclear binding energy

Mass parabolas for constant A

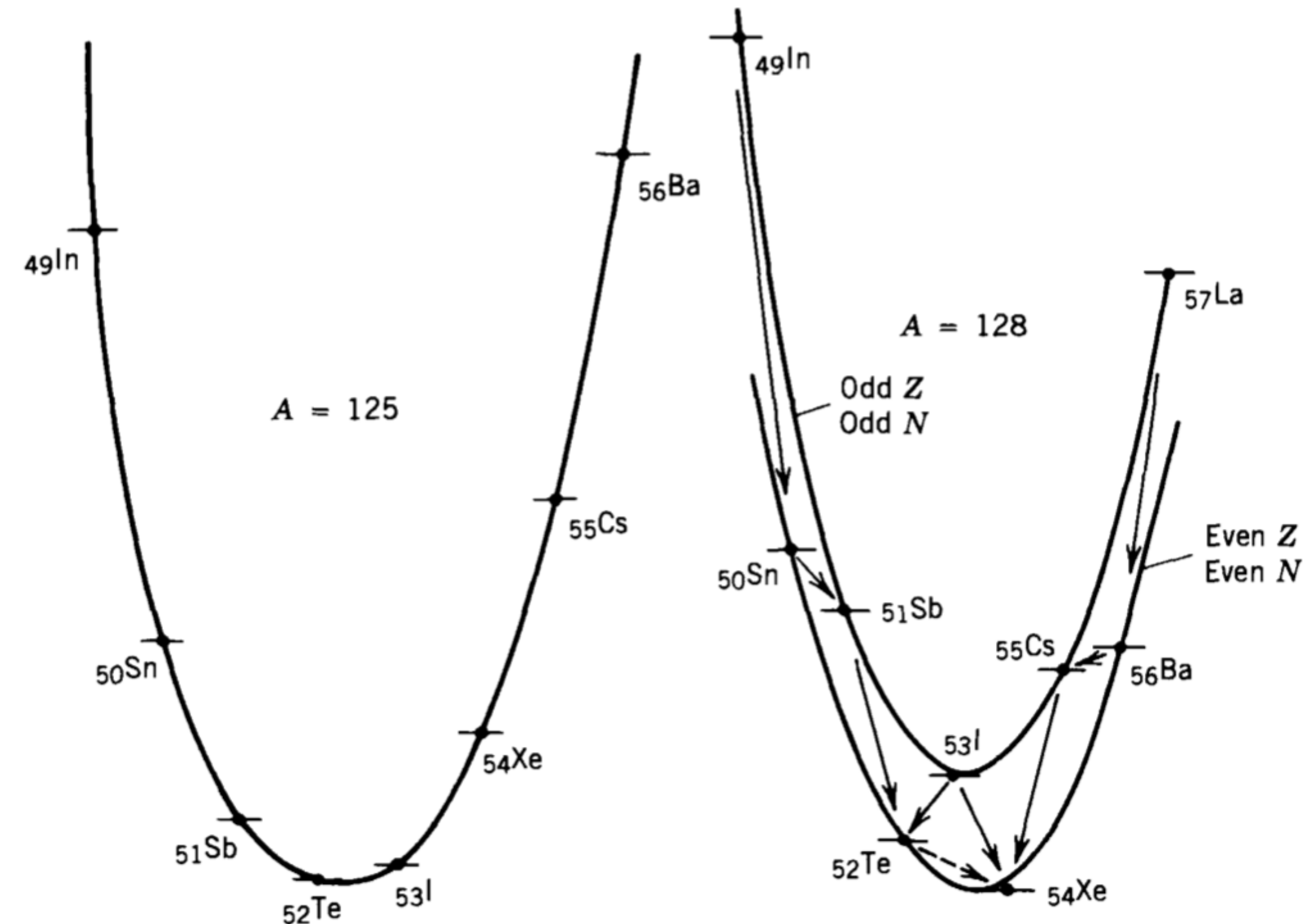


Figure 3.18 Mass chains for $A = 125$ and $A = 128$. For $A = 125$, note how the energy differences between neighboring isotopes increase as we go further from the stable member at the energy minimum. For $A = 128$, note the effect of the pairing term; in particular, ^{128}I can decay in either direction, and it is energetically possible for ^{128}Te to decay directly to ^{128}Xe by the process known as double β decay.